

Integrating Two Haptic devices for Performance Enhancement

Enzo Pasquale Scilingo Nicola Sgambelluri Giovanni Tonietti Antonio Bicchi

Interdepart. Research Center "E. Piaggio", University of Pisa, via Diotisalvi, 2, Pisa, Italy

E-mail: e.scilingo@ing.unipi.it, n.sgambelluri@ing.unipi.it, g.tonietti@ing.unipi.it, bicchi@ing.unipi.it

Abstract—This paper deals with a new configuration for a haptic system, which is able to simultaneously replicate independent force/displacement and force/area behaviors of a given material. Being force/area information a relevant additional haptic cue for improving softness discrimination, this system allows to extend the range of materials whose rheology can be carefully mimicked. Moreover, according to the Hertz theory, two objects with different curvature radius having the same force/displacement behavior can respond with different contact area to the same applied force. These behaviors can be effectively replicated by the integrated haptic system here proposed enabling and independent control of force/displacement and force/area. The system is comprised of a commercial device (Delta Haptic Device) serially coupled with a Contact Area Spread Rate (CASR) device. Two specimens of a material and two of another one, all with different curvature radii, were identified and modeled in terms of force/area and force/displacement. These behaviors were successfully tracked by the integrated haptic system here proposed.

I. INTRODUCTION

Human capability of tactually discriminating softness involves many perceptual aspects and is mediated by both kinesthetic and cutaneous receptors laying in the skin. In order to enhance performance of a haptic display, both these channels should be elicited [3]. In literature several attempts to implement devices capable of providing, in addition to kinesthetic information, cutaneous information, e.g. by means of shape and/or vibration feedback, or conveying thermal data can be found [7], [8], [9]. Here, we propose a new configuration of haptic interface based on the mechanical coupling of two technologies. The first one refers to a new conjecture, first proposed by [1], [2], based on surrogating detailed tactile information for softness discrimination with information on the rate of spread of the contact area between the finger and the object as the contact force increases. This conjecture relies on the paradigm that a large part of haptic information necessary to discriminate softness of objects by touch is contained in the law that relates resultant contact force to the overall area of contact, or in other terms in the rate by which the contact area spreads over the finger surface as the finger is increasingly pressed on the object. Authors called this relationship Contact Area Spread Rate (CASR). Clearly, such a conjecture only suggests that, in the lack of better resources, the CASR information might be an acceptable surrogate for the complete sense of touch, to increase the tactile perception, but it does not pretend to minimize the importance of other relevant aspects of tactile information, such as, e.g., shape of the contact zone

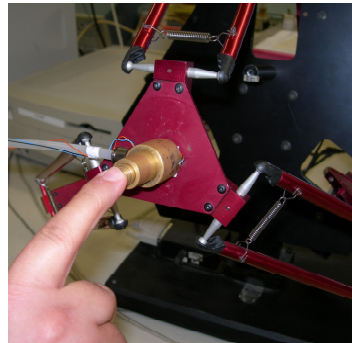


Fig. 1. Picture showing the haptic system.

or pressure distribution in the contact area. For the sake of citation, next works [10] presented a softness display based on the control of fingertip contact area, although it was not able to display the dynamic change of the contact area and did not have enough spatial resolution. The CASR display, which mainly address cutaneous channels [5], is mechanically coupled with a commercial device, the Delta Haptic Device (DHD) by Force Dimension [4]. This paper aims at experimentally verify if this combination is able to constructively join the advantages of each device improving the overall performance. Indeed, the CASR device is able to provide careful force/area and force displacement relationships, but due to mechanical constraints, these two behaviors are intimately related. On the other hand, the DHD can reliably provide force/displacement behavior, but it is not able to reproduce force/area. Combining the two devices, therefore, we can independently control force/area and force/displacement curves, thus extending the range of materials which can be reproduced. In addition, there are some materials which have the same force/displacement relationship, but different force/area curve (this latter, indeed, strongly depends on the geometry) and only an independent control of the two behaviors can replicate a similar rheology.

II. THE HAPTIC SYSTEM

The haptic system here proposed is comprised of a CASR display [1] placed on the top of the Delta Haptic Device (DHD) (see Fig.1. The CASR display is a pneumatic device consisting of a set of cylinders of different radii in telescopic arrangement (see right side of Fig.2). A regulated air pressure

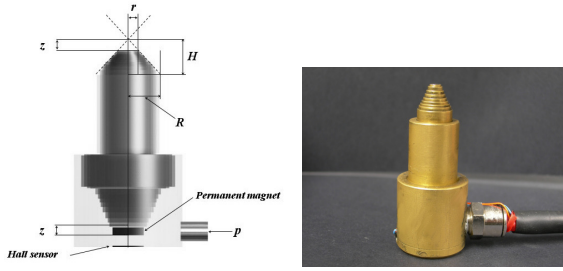


Fig. 2. Schematic view (left) and picture (right) of the CASR display.

is inflated inside the display and acts on the cylinders so as to provide a simulated compliance which can be perceived by the operator when pushing with their forefinger against the top of the display. The schematic view of the CASR display is shown in the left side of fig.2. A proportional Hall sensor placed at the bottom of the inner chamber allows to measure the displacement z of the cylinders when the subject pushes against them, while a servo pneumatic actuator regulates the chamber pressure according to the desired CASR profile to replicate. The DHD is a commercial interface, widely used by the haptic research community. It is a high performance haptic device and has 6 degrees of freedom: 3 translations from the parallel Delta structure and 3 rotations from a wrist module. Unlike other haptic mechanisms having either limited force capability or small workspace, the DHD is capable of providing large forces (up to 25N) over a large volume (30 cm diameter, 30 cm length). In addition, because of its design and its base-mounted actuators, the device offers high stiffness, decoupled translation and rotation, as well as very low inertia. The haptic system exploits both performance of the two devices, joining the high fidelity and quality of tactile information of the CASR to the large workspace and high stiffness of the DHD.

III. MOTIVATION

The initial contact of a mechanical interaction between two bodies may occur at a point in case of spherical geometry or along a line in case of cylindrical bodies [6]. Let us focus on spherical geometry. Applying a slight load the area around the initial contact point begins deforming. In such a way the mechanical interaction takes place on a finite smaller area than bodies dimensions. Contact theory predicts the shape of contact area and its behavior with time and with increasing load. Moreover, it allows to identify stress and strain components in both bodies within and outside the loaded area. Let us take a rectangular coordinate system with the origin as point of first contact in which the x-y plane is the common tangent plane the two surfaces (see fig.3). Let us consider two points S_1 e S_2 on the surface of the two bodies having coordinates $S_1(x, y, z_1)$ e $S_2(x, y, z_2)$ before loading. The distance between them is given by:

$$h = z_1 - z_2 = \frac{1}{2} \left(\frac{1}{R_1'} + \frac{1}{R_2'} \right) x^2 + \frac{1}{2} \left(\frac{1}{R_1''} + \frac{1}{R_2''} \right) y^2 = \frac{1}{2R'} x^2 + \frac{1}{2R''} y^2 = Ax^2 + By^2 \quad (1)$$

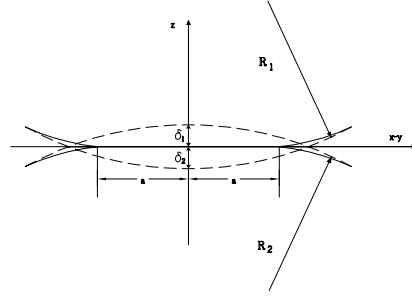


Fig. 3. Geometry of the contact area when two bodies come into contact.

where A e B are positive constants, R' and R'' are defined as the principal relative radii of curvature.

It is possible to combine the previous radii introducing an equivalent radius of curvature defined as $R_e = \sqrt{R'R''} = \frac{1}{2} \sqrt{\frac{1}{AB}}$.

From equation 1 the profile of the distance h constant between unstrained surfaces are elliptical. When two bodies are brought into contact, distant points T_1 e T_2 move towards the origin O in parallel direction to axis z by displacements equal to δ_1 e δ_2 respectively. The contact pressure produces on the surface of each body a deformation in parallel direction to axis z by an amount u_{z1} e u_{z2} (positively measured within each body). If after loading S_1 e S_2 are coincident within the contact surface, then we can write:

$$\bar{u}_{z1} + \bar{u}_{z2} + h = \delta_1 + \delta_2 \quad (2)$$

Assuming $\delta = \delta_1 + \delta_2$ and substituting h by 1, the equation 2 becomes

$$\bar{u}_{z1} + \bar{u}_{z2} = \delta - Ax^2 - By^2 \quad (3)$$

If S_1 e S_2 , after loading, are outside the contact area then

$$u_{z1} + u_{z2} > \delta - Ax^2 - By^2$$

In the equations 1, if the two bodies coming into contact are solids of revolution then $R_1' = R_1'' = R_1$; $R_2' = R_2'' = R_2$, hence the equation 1 gets as:

$$h = z_1 - z_2 = \frac{1}{2R_1} x^2 + \frac{1}{2R_1} y^2 + \frac{1}{2R_2} x^2 + \frac{1}{2R_2} y^2 = \frac{1}{2} \left(\frac{1}{R_1} + \frac{1}{R_2} \right) x^2 + \frac{1}{2} \left(\frac{1}{R_1} + \frac{1}{R_2} \right) y^2$$

which can be rewritten as

$$h = Ax^2 + By^2$$

obtaining

$$A = B = \frac{1}{2} \left(\frac{1}{R_1} + \frac{1}{R_2} \right)$$

Substituting

$$\frac{1}{R} = \frac{1}{R_1} + \frac{1}{R_2}$$

and writing it in polar coordinates ($x^2 + y^2 = r^2$) the equation 3 becomes

$$\bar{u}_{z1} + \bar{u}_{z2} = \delta - \frac{1}{2R} r^2 \quad (4)$$

When two spherical solids come into contact, the initial contact occurs at a single point which spreads over a circular area. According the Hertz theory [6] the pressure exerted onto a generic circular area having radius r within the contact area between two solids of revolution is

$$p(r) = \frac{p_0}{a} \sqrt{(a^2 - r^2)}, \quad r \leq a$$

where a is the radius of the circular contact area.

The total pressure is

$$P = \int_0^a p(r) 2\pi r dr = \frac{2}{3} p_0 \pi a^2.$$

Let us introduce the equivalent quantity

$$\frac{1}{E^*} = \frac{1 - \nu_1^2}{E_1} + \frac{1 - \nu_2^2}{E_2}$$

where E_1 , E_2 , ν_1 and ν_2 are the Young modulus and Poisson ratio for the two bodies coming into contact, respectively.

The equation 4 can be rewritten as:

$$\frac{\pi p_0}{4aE^*} (2a^2 - r^2) = \delta - \frac{1}{2R} r^2 \quad (5)$$

where substituting $r = a$ we can obtain the radius of contact area:

$$a = \frac{\pi p_0 R}{2E^*} \quad (6)$$

From this latter equation, it is worthwhile noting that Young modulus, contact area and curvature radius are strictly and intimately correlated. Young modulus relates the applied force (stress) with the induced displacement (strain). Eq. 6 says that if two bodies are constitutively made of the same material, hence they have the same Young modulus, i.e. the same force/displacement, but different curvature radius, then they have different force/area behavior.

In order to replicate the rheology of these materials, it is necessary to implement an independent control of force/displacement and force/area.

CASR display is able to replicate force/area behaviors with high reliability from a perceptual point of view, but it does not allow to implement two independent profiles of force/area and force/displacement. Indeed, when an external force is applied on the device it returns a reaction force given by $F = PA(z)$, where P is the pressure inflated into the inner chamber of the display and $A(z)$ is the contact area. This latter, however, is strictly related to the normal displacement by the bijective relationship $A(z) = \pi \frac{z^2 R^2}{H^2}$, where z is the normal displacement, R is the cylinder radius and H is the height of the cone (see Fig.2). Therefore, when a force/area profile is set, force/displacement is indirectly obtained. On the other hand, DHD is a haptic interface which enables to reliably replicate force/displacement curves, but it does not allow to provide force/area behavior. Coupling the two devices, it is possible to control independently force/area and force/displacement, joining synergistically the two performance.

IV. HARDWARE EQUIPMENT: MODELING AND IDENTIFICATION

In this section, we modeled the CASR device in order to analytically characterize it in terms of force/area parameterized with the pressure. Afterwards, these curves were experimentally validated inflating inside the CASR device progressive constant pressures and measuring force/area profile at each pressure.

A. Theoretical model of CASR display

If we assume the system lossless, while the probing finger pushes with a constant force F against the top of the display, this latter exerts an equal and opposite reaction at the equilibrium position in agreement with the virtual work principle:

$$F \delta z = -p \delta V \Rightarrow F = -p \frac{\delta V}{\delta z}, \quad (7)$$

where δz and δV are respectively the virtual displacement along the z axis, and the virtual variation of the volume V of the CASR display. The variation of the inner volume of the CASR display is given by

$$\delta V = -\pi \frac{z^3 R^2}{3H^2},$$

in which $H = 0.01$ m is the maximum height, and $R = 0.0065$ m is the radius calculated at the basis of the CASR display. According to eq.7, we easily obtain the analytical model for the display

$$F = p \pi \frac{z^2 R^2}{H^2} = p A. \quad (8)$$

B. Experimental model of CASR display

The analytical model previously calculated has been experimentally assessed using the hardware setup shown in fig.4. The CASR display was submitted to indentation tests at different pressures by means of a compressional indenter driven by an electromagnetic mini-shaker. The actuator, made by Bruel & Kjaer, is a linear current step motor mini-shaker type, capable of applying a maximum displacement of 10 mm in axial direction. The indenter is a metallic cylinder of 1.5 cm in diameter and 10 cm in length. The indenter is equipped with a magnetic linear transducer, Vit KD 2300/6C by KAMAN Science Corporation, used to measure the applied axial displacement and with a load cell sensor, ELH-TC15/100 by Entran, able to detect forces up to ± 50 N.

An external electronic driver is used to activate the indenter and acquire force-position signals from the sensors.

A data acquisition PCI card with one analog output channel and two analog input channels, is used to gather signals and sent them to a PC. A dedicated software was implemented in Matlab/Simulink environment to control in feedback and in real-time the displacement of the indenter and record and plot the signals.

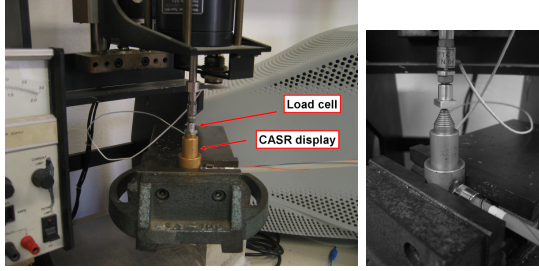


Fig. 4. Experimental setup used for identifying the CASR model (on the left side). On the right side a zoom view of the system is reported.

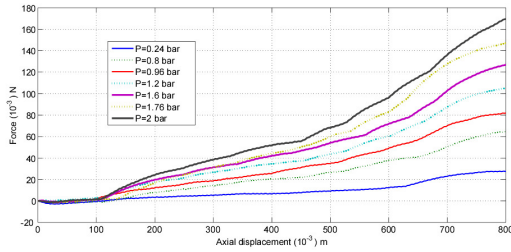


Fig. 5. Force/Displacement response of the prototype CASR display at increasing values of constant pressure.

C. Identification assessment

In fig.5 experimental curves of force versus axial displacement of the CASR display at different values of pressure are reported. Keeping the pressure constant, as the shaker pushes onto the CASR the outputs from both force and position sensor are recorded. The pressure inside the display is maintained constant as the shaker pushes by an internal control of a servovalve, Proportion-Air's QB series, employed to this purpose. The experimental curves were compared with the theoretical ones. In fig.6 three experimental force/area curves at three different values of pressure were compared with the corresponding theoretical ones. Results are very satisfactory.

Fig.6 shows a satisfactory agreement between three any CASR force/displacement curves and those theoretically calculated at the same pressures. This means that the air loss inside the CASR display can be considered negligible.

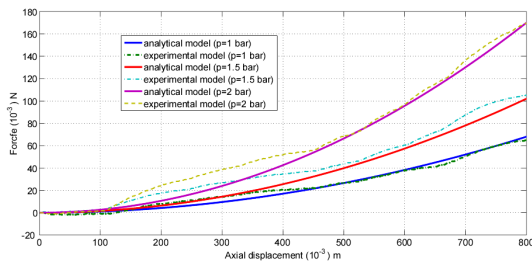


Fig. 6. Force/Displacement response of the CASR display compared with the analytical model at three different levels of pressure, by way of illustration.

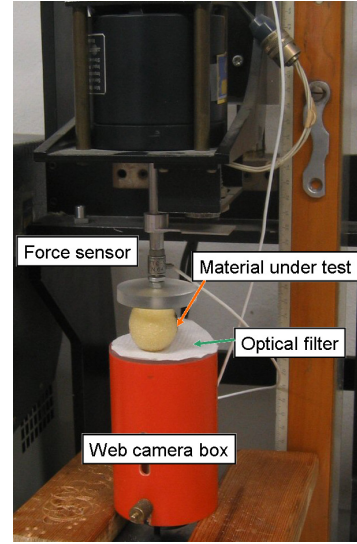


Fig. 7. Experimental setup used for identifying force/area curve of the specimens.

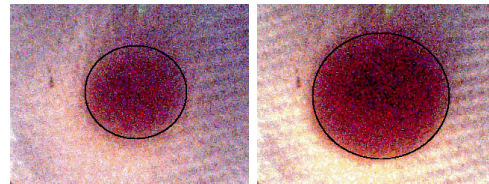


Fig. 8. Two different snapshots of the contact area captured on the same specimen having radius $R = 1.3cm$ at two level of force.

V. EXPERIMENTAL

Two sphere-shaped viscoelastic specimens, M_1 and M_2 , approximately homogeneous and with different curvature radius were selected to be submitted to an experimental protocol where both force-area and force-displacement curves are acquired. Fig.7 shows the experimental setup used to acquire force/area curves. The same hardware setup used for characterizing the CASR display was additionally equipped with a dedicated area sensor. The specimen was positioned onto a transparent plexiglass surface whereunder a web camera was placed. As the indenter pushes against the specimen the web cam captures a snapshot of the surface flattened against the plexiglass. In order to enhance contours of contact area a thin white paper behaving as optical filter was placed between the specimen and the plexiglass. In addition to force/area, also the indentation depth is detected by a magnetic position sensor. In fig.V two snapshots of the contact area were captured on the same specimen at two different level of indenting force are shown. The experimental force/area curves acquired by the hardware setup previously described as well as the corresponding mathematical interpolated curves are reported in fig.9 for the two specimens. A quadratic interpolation provided best fitting.

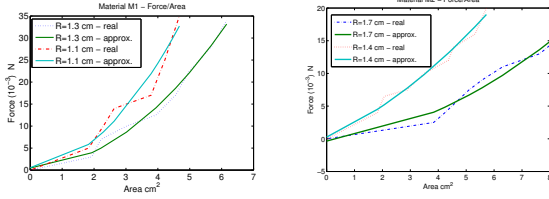


Fig. 9. Experimental force/area and interpolated curves for two sphere-shaped specimens of the same material M_1 having radius ($R = 1.3\text{cm}$ and $R = 1.1\text{cm}$) on the left side and M_2 having radius ($R = 1.7\text{cm}$ and $R = 1.4\text{cm}$) on the right side

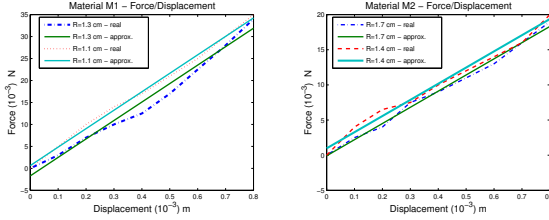


Fig. 10. Force/Displacement and approximations of spherical specimen M_1 having different radius ($R = 1.3\text{cm}$ and $R = 1.1\text{cm}$) on the left side and M_2 having different radius ($R = 1.7\text{cm}$ and $R = 1.4\text{cm}$) on the right side.

Two spherical specimens of the same material M_1 , having radius $R = 1.1\text{ cm}$ and $R = 1.3\text{ cm}$, respectively, and two specimens of the material M_2 having radius $R = 1.4\text{ cm}$ and $R = 1.7\text{ cm}$ were characterized in terms of force/area and force/displacement. Experimental curves of force/area were interpolated and as expected from the Hertz theory best fitting was obtained by a quadratic interpolation. These equation were used in the control law. Here we report, by way of illustration, the interpolated equation for the specimen of radius $R = 1.1\text{ cm}$ of the material M_1 :

$$F(A)|_{(M_1, R=1.1)} = 1.4A^2 + 0.33A + 0.55 \quad (9)$$

Fig.9 show all the four experimental force/area curves along with the interpolated ones. An analogous procedure was done for force/displacement identification. Results are reported in fig.10 left and right. As it can be seen, these curves are mathematically approximated by a linear interpolation.

For the sake of brevity, here we report the equation of the interpolated curve for the specimen of material M_2 with radius $R = 1.4\text{cm}$

$$F(z)|_{(M_2, R=1.4)} = 23z + 0.97 \quad (10)$$

It is worthwhile noting that the slope of the interpolated curves for the same material is the same, in agreement with the theory that same materials, though with different geometry, have same Young modulus, hence roughly the same force/displacement curves.

A. Control strategy

The integrated haptic system here proposed allows to replicate any force/area and force/displacement behaviors,

thanks to the possibility of independently controlling the displacement z_D of the DHD in addition to the air pressure p inflated inside the CASR device. If we denote, indeed, z_C and z_D the displacements of the CASR and of the DHD respectively, both force/area and force/displacement behaviors can be mapped by the independent set of controls p and $z_D = z_m - z_C$, where z_m is the material displacement to replicate.

Let us suppose to replicate, e.g., the material M_1 , neglecting in force/area equation the terms of zero and first order and neglecting the intercept in the straight-line equation of force/displacement.

$$\begin{cases} F_m = \alpha_m A_m^2 \\ z_m = \beta_m F_m \end{cases} \quad (11)$$

The behavior force/area should be reproduced by the CASR device, whose force/area characteristic is reported in 8. Imposing the same force and area of the material to replicate, we get

$$p = \alpha_m A_m \quad (12)$$

In order to track the force/displacement behavior, we should set

$$z_m = z_C + z_D \quad (13)$$

where z_C is read by the position sensor placed inside the CASR display and is analytically given by the combination of 8 and 12.

Being the two devices mechanically coupled in series, we have $F_C = F_D$ which in turn should be equal to F_m . This force is the input of DHD, while the output z_D is controlled in feedback so that $z_D = z_m - z_C$ which can be expressed as

$$z_D = z_m - z_C = \beta_m F_m - z_C = \beta_m p \frac{\pi R^2}{H^2} z_C^2 - z_C \quad (14)$$

VI. EXPERIMENTAL RESULTS

In order to assess the performance of the control strategy, we replicated the behavior of the materials M_1 and M_2 , previously identified. Pushing on the haptic system with a desired force profile, the control law responded in terms of area and displacement in agreement with the analytical model of materials previously identified. Output from area and displacement sensors of the haptic system were compared with the analytical desired trajectories and we reported experimental results in Figs. 11, 12, 13, and 14. As it can be seen, our system is able to successfully track the theoretical curves with negligible errors. In addition to good tracking performance, our combined system is also able to provide increased haptic feeling and further psychophysical experiments aiming at assessing that are planned to be performed. This confidence is supported by results from previous works [1]. Indeed, in the new combined system here proposed, cutaneous information is mostly provided by the CASR display which was already shown to better discriminate softness with respect to a purely kinaesthetic display but additionally kinaesthetic information is increasingly enhanced by DHD performance, in terms of accuracy and reliability.

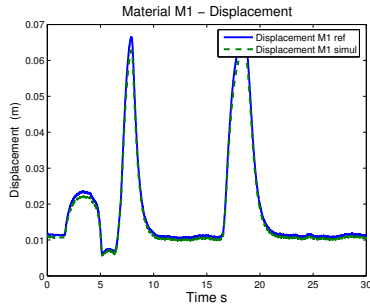


Fig. 11. Tracking of the displacement of M_1 by the haptic system. Continuous line represents the response of the model of the material to an external force, while dashed line is the tracking output of the system.

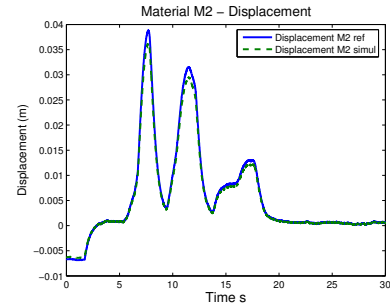


Fig. 13. Tracking of the displacement of M_2 by the haptic system. Continuous line represents the response of the model of the material to an external force, while dashed line is the tracking output of the system.

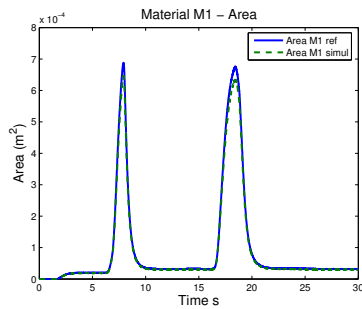


Fig. 12. Tracking of the area of M_1 by the haptic system while an external force is applied. Continuous line represents the response of the model of the material, while dashed line is the tracking output of the system.

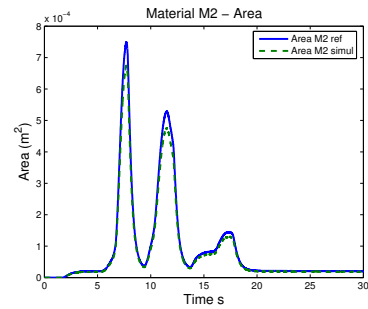


Fig. 14. Tracking of the displacement of M_2 by the haptic system while an external force is applied. Continuous line represents the response of the model of the material, while dashed line is the tracking output of the system.

VII. CONCLUSION

In this paper we proposed a new configuration of haptic system comprised of two devices mechanically coupled in series. This new architecture allowed to implement an independent control of force/area and force displacement, extending the range of materials which can be replicated. After introducing theoretical motivation led us to this new approach, we identified four specimens consisting in two materials, M_1 and M_2 each one of two different sizes. The two specimens having different geometry of the same material M_1 exhibit the same force/displacement, but different force/area. They can be replicated only by a device able to implement an independent control of the two behaviors. The same is true of the material M_2 . Experimental results showed that the new system here proposed is able to effectively track every curve of each material.

VIII. ACKNOWLEDGMENT

This research is partially funded by the EU Commission under contract IST-4-027141 Immersence.

REFERENCES

[1] A. Bicchi, D. De Rossi, and E. P. Scilingo. The Role of Contact Area Spread Rate in Haptic Discrimination of Softness. *IEEE Trans. on Robotics and Automation*, 16(5):496-504, October 2000.

[2] A. Bicchi, E.P. Scilingo, D. Dente, and N. Sgambelluri. Tactile Flow and Haptic Discrimination of Softness. In *Multi-point Interaction with Real and Virtual Objects*, Springer Tracts in Advanced Robotics, (18):165-176, 2005.

[3] D.G. Caldwell, S. Lawther, and A. Wardle, "Multi-Modal Cutaneous Tactile Feedback", In *Proc. of the IEEE/RSJ International Conference on Intelligent Robots and Systems IROS*, pages 465-472, Osaka, Japan, 1996.

[4] www.forcedimension.com

[5] E. B. Goldstein, "The Cutaneous Senses" Ch.14, *Sensation and Perception*, 3rd Ed., Wadsworth Publishing Company (Belmont CA, reprinted 1989).

[6] K. L. Johnson, "Contact mechanics", Cambridge University Press. 1985, Chapter 4.

[7] V. Hayward, O. R. Astley, M. Cruz-Hernandez, D. Grant, G. Robles-De-La-Torre, "Haptic Interfaces and Devices", *Sensor Review*, 24(1), Feb. 2004

[8] H. Yano, K. Komine, H. Iwata, "Development of a High-resolution Surface Type Haptic interface for Rigidity Distribution Rendering" Page(s): 355- 360, In *Proc. First World Haptics Conference*, Pisa, Italy.

[9] M. A. Srinivasan and R. H. LaMotte, "Tactile Discrimination of Softness", *Journal of Neurophysiology*, Vol. 73, No. 1, pp. 88-101, Jan 1995.

[10] K. Fujita, H. Ohmori, "A New Softness Display Interface by Dynamic Fingertip Contact Area Control", *Proc. of the 5th World Multiconference on Systemics, Cybernetics and Informatics*, 78-82, 2001.